Biometals (2008) 21:239–248
DOI 10.1007/s10534-007-9112-9

An investigation of hemopexin redox properties by spectroelectrochemistry: biological relevance for heme uptake

Meghan M. Flaherty · Kimberley R. Rish · Ann Smith · Alvin L. Crumbliss

Received: 5 July 2007 / Accepted: 26 July 2007 / Published online: 22 August 2007

Abstract Hemopexin (HPX) has two principal roles: it sequesters free heme in vivo for the purpose of preventing the toxic effects of this moiety, which is largely due to heme's ability to catalyze free radical formation, and it transports heme intracellularly thus limiting its availability as an iron source for pathogens. Spectroelectrochemistry was used to determine the redox potential for heme and meso-heme (mH) when bound by HPX. At pH 7.2, the heme-HPX assembly exhibits $E_{1/2}$ values in the range 45–90 mV and the mH-HPX assembly in the range 5–55 mV, depending on environmental electrolyte identity. The $E_{1/2}$ value exhibits a 100 mV positive shift with a change in pH from 7.2 to 5.5 for mH-HPX, suggesting a single proton dependent equilibrium. The $E_{1/2}$ values for heme-HPX are more positive in the presence of NaCl than KCl indicating that Na^+, as well as low pH (5.5) stabilizes ferro-heme-HPX. Furthermore, comparing KCl with K_2HPO_4, the chloride salt containing system has a lower potential, indicating that heme-HPX is easier to oxidize. These physical properties related to ferri-/ferro-heme reduction are both structurally and biologically relevant for heme release from HPX for transport and regulation of heme oxygenase expression. Consistent with this, when the acidification of endosomes is prevented by bafilomycin then heme oxygenase-1 induction by heme-HPX no longer occurs.

Keywords Heme · Meso-heme · Hemopexin · Iron · Hemophore · Heme transport · Redox · Endocytosis

Abbreviations

DMEM	Dulbecco's Minimal Essential Medium
HEPES	4-(2-hydroxyethyl)-1-piperazine ethanesulfonic acid
H	Heme, protoporphyrin-IX
HO-1	Heme oxygenase-1
HPX	Hemopexin
mH	Meso-heme
NHE	Normal hydrogen electrode
OTTLE	Optically transparent thin-layer electrode
SDS	Sodium dodecyl sulfate

M. M. Flaherty · A. L. Crumbliss (✉)
Department of Chemistry, Duke University,
Box 90346, Durham, NC 27708-0346, USA
e-mail: Alvin.crumbliss@duke.edu

K. R. Rish · A. Smith
Division of Molecular Biology and Biochemistry, School of Biological Sciences, University of Missouri – K.C., Kansas City, MO 64110-2499, USA

Introduction

Heme cofactors in biological systems are essential to carry out a variety of functions, including a cascade of reactions such as: electron transport (e.g., cytochromes); serving as the active site of oxygen

carrying molecules (e.g., the globins: hemoglobin, myoglobin, and neuroglobins) and diatomic gas binding heme sensors (e.g., the bacterial FixL and CooA receptors); mammalian transcription factors (including NPAS2, a circadian rhythm regulator, and Bach1); drug metabolizing enzymes (e.g., cytochrome P-450 family of enzymes); anti-oxidant and detoxifying enzymes (e.g., peroxidases like catalase); and many other enzymes (e.g., nitric oxide synthases, guanylyl cyclases). Yet the presence of a free heme group can be toxic to cells and lead to oxidative damage (Halliwell and Gutteridge 1986). Hemopexin (HPX) is a glycoprotein that by sequestration scavenges the heme groups that are liberated from hemoglobin during hemolysis and from other cellular heme-proteins, thus controlling heme-facilitated cellular oxidation while maintaining the solubility of lipophilic heme in its monomeric form (Genco and Dixon 2001; Morgan and Smith 2001; Ascenzi et al. 2005). Unusual interrelationships between the heme-binding HPX and hemoglobin-binding haptoglobin are revealed in HPX null mice (Tolosano et al. 1999, 2002). While hemoglobin can mediate oxidative damage during intravascular hemolysis, it is only a weak peroxidase, whereas the heme that is liberated from hemoglobin is a highly reactive molecule. Thus, HPX is the first line of defense against the oxidative stress from heme in hemolysis, trauma and reperfusion injury.

After intravenous injection of [^{59}Fe]heme-HPX, the complex is taken up principally by epithelial cells, including hepatic parenchymal cells (Smith and Morgan 1978, 1979), via endocytosis (Smith and Hunt 1990). HPX, isolated as described here, co-localizes with transferrin, the paradigm for recycling receptors (Smith and Hunt 1990), and, significantly, also recycles intact from the liver of intact rats[7,8] and from cultured HepG2 cells (Smith and Hunt 1990). Subsequently, the heme released from HPX intracellularly is rapidly degraded by heme-oxygenase, an enzyme of the smooth endoplasmic reticulum, and its iron stored in ferritin (Davies et al. 1979). Heme catabolism produces ferrous iron, biliverdin and carbon monoxide that are released into the cytoplasm. In the circulation or cellular fluids, as well as during the HPX transport/recycling process, HPX controls the heme-catalyzed oxidation by both regulating the redox potential at the heme-iron [Fe(III)/Fe(II)-protoporphyrin IX] center and by making the heme physically inaccessible for catalysis.

The chemistry and biochemistry of HPX has been reviewed (Morgan and Smith 2001; Ascenzi et al. 2005) and a crystal structure is available (Faber et al. 1995; Paoli et al. 1999). HPX has one of the highest affinities for heme (K_d less than pM, Hkal et al. 1974) and at a plasma concentration of 0.5–1.2 mg/ml (*ca.* 20 μM) it effectively competes (Morgan et al. 1976) with human serum albumin (HSA, 35–55 mg/ml plasma) with one high affinity heme binding site of $K_d \sim 10$ nM and two lower affinity sites with $K_d \sim 1$ μM (Beaven et al. 1974). HPX not only transports heme, but also acts as an extracellular antioxidant (Gutteridge and Smith 1988) protecting cells and circulating molecules, e.g., low density lipoproteins, from heme-mediated oxidation (Miller et al. 1996). The binding of a single heme molecule by HPX occurs via bis-histidyl protein side chain coordination (Faber et al. 1995; Paoli et al. 1999); HPX is highly conserved and many of its physicochemical properties have been well characterized (Morgan and Smith 2001).

Spectroelectrochemical investigation of the heme-HPX complex as reported here provides insight into: (1) the role of HPX in controlling the reduction potential of the heme iron center; (2) the influence of bis-histidyl coordination at the heme iron center; and (3) the possible role of heme iron redox in the HPX-mediated transport and release of heme from the tight binding site on HPX for catabolism and gene regulation. A brief report, published nearly 30 years ago, determined an $E_{1/2}$ for heme-HPX (+65 mV) using redox titration methods at pH 7 (Hkal et al. 1977). Here, we investigate further the redox properties of naturally occurring heme (iron-protoporphyrin IX) bound to HPX (H-HPX) and a second HPX complex containing meso-heme (mH-HPX) with a heme analog in which the vinyl side chains of protoporphyrin IX are replaced by ethyl groups. Spectroelectrochemistry experiments are reported as a function of pH and background electrolyte that are physiologically relevant. mH-HPX has been shown to act in a biological manner similarly to H-HPX (Smith and Morgan 1979, 1981, 1984). However, the atomic structure of heme and heme analogs may subtly influence redox parameters of heme-HPX complexes and there is evidence that heme-HPX stimulates cell surface events including the participation and activation of electron transport processes (Eskew et al. 1999; Sung et al. 2000; Vanacore et al. 2000).

Heme-HPX complexes in biological fluids, like plasma, play an important role in vivo. We show here how new biophysical information on heme-HPX is related to its biological functions and regulatory consequences in mammalian cells.

Materials and methods

Preparation of heme (iron-protoporphyrin IX)-hemopexin (H-HPX) and meso-heme (iron-mesoporphyrin IX)-hemopexin (mH-HPX)

Hemopexin was isolated from trace-hemolyzed rabbit plasma using differential precipitation and ion-exchange chromatography as previously described (Morgan et al. 1993). After purification, the HPX was dialyzed against 5 mM sodium phosphate buffer, pH 7.4 at 4°C before lyophilization. The purity of apo-HPX was established by Sodium dodecyl sulfate-polyacrylamide gel electrophoresis (SDS-PAGE; Amersham Biosciences miniVE system®, Piscataway, NJ, USA) using 4–20% acrylamide gradient gels. Following this isolation the protein is fully sialylated, as was the source of HPX from which the 3D structure has been determined (Paoli et al. 1999). HPX specifically and tightly binds 1 equivalent of heme with characteristic changes in the circular dichroism spectra (Seery et al. 1975). The protein prepared in this way is not toxic to cells and is fully active in heme transport in vivo (Smith and Morgan 1978, 1979), activation of signaling cascades (Smith et al. 1997; Eskew et al. 1999; Vanacore et al. 2000) and gene regulation (Alam and Smith 1989, 1992), is recycled rather than extensively degraded (Smith and Morgan 1978, 1979, 1990), and when iodinated has a plasma half-life of at least ~37 h (Conway et al. 1975; Liem et al. 1975; Morgan et al. 1988), characteristic of native plasma proteins. To form the H-HPX or mH-HPX complex, the lyophilized apo-HPX was dissolved in a solution of ice-cold 10 mM sodium phosphate (PBS; Sigma Chemical Company, St. Louis, MO) and 0.15 M NaCl (pH = 7.35; Fisher Scientific, Horsham, PA). The buffer was added dropwise to the protein until a final concentration of 11 mg/ml was obtained. Concurrently, a solution of 4 mM heme [iron-protoporphyrin IX (H), or iron-mesoporphyrin (mH)] was made using dimethylsulfoxide (DMSO; Fisher Scientific). To avoid protein denaturation, the DMSO concentration in the complex is kept below 5% (Morgan and Smith 1984; Morgan et al. 1988; Shipulina et al. 2001). The heme and protein solutions were then mixed in a 9:10 molar ratio. To ensure complete formation of the 1:1 heme-HPX complexes, a spectrum was obtained 20 min after mixing and the absorbance values for the protein and Soret bands were compared (protein λ_{max} = 280 nm, $\varepsilon_{280} = 1.1 \times 10^5$ M^{-1} cm^{-1}; Soret bands for ferri-H-HPX, λ_{max} = 413 nm, $\varepsilon_{413} = 1.1 \times 10^5$ M^{-1} cm^{-1}; ferri-mH-HPX, λ_{max} = 405 nm, $\varepsilon_{405} = 1.3 \times 10^5$ M^{-1} cm^{-1} (Morgan and Muller-Eberhard 1972).

The H-HPX and mH-HPX were extensively dialyzed against PBS and 4-(2-hydroxyethyl)-1-piperazine ethanesulfonic acid (HEPES) buffers using Pierce Scientific disposable 10 K MWCO Slide-A-Lyzer Dialysis Cassettes. After dialysis was complete, the concentration of the protein was checked spectroscopically. If concentration of the protein sample was necessary Amicon Bioseparations Centricon® Plus-20 centrifugal filter devices were used. Once the protein was in the correct buffer system and was at the right concentration, aliquots were snap-frozen under liquid nitrogen until needed for experimental purposes.

Spectroscopic characterization of H-HPX and mH-HPX

The Soret band molar absorptivities of the oxidized species are as follows: $\varepsilon_{413} = 1.1 \times 10^5$ M^{-1} cm^{-1} (H-HPX) and $\varepsilon_{405} = 1.3 \times 10^5$ M^{-1} cm^{-1} (mH-HPX) (Morgan and Muller-Eberhard 1972). The Soret band molar absorptivities of the reduced species are as follows: $\varepsilon_{428} = 1.45 \times 10^5$ M^{-1} cm^{-1} (H-HPX) and $\varepsilon_{414} = 1.6 \times 10^5$ M^{-1} cm^{-1} (mH-HPX) (Morgan and Muller-Eberhard 1972). Other maxima were observed for ferro-H-HPX at 526 and 556 nm and ferro-mH(FeII)-HPX at 520 and 550 nm as previously published (Morgan and Muller-Eberhard 1972; Morgan and Smith 2001).

Spectroelectrochemistry

Spectroelectrochemical measurements of the redox midpoint potentials ($E_{1/2}$) of H-HPX and mH-HPX

were made using an optically transparent thin layer electrode (OTTLE) and an experimental configuration that is described elsewhere (Taboy et al. 2002; Dhungana and Crumbliss 2007). The apparatus was calibrated using sperm whale myoglobin, which gave results consistent with those reported in the literature. All $E_{1/2}$ values are reported relative to the normal hydrogen electrode (NHE). A typical spectroelectrochemistry experiment used 0.1 mM protein, 2.5 mM $K_3Fe(CN)_6$ mediator, 500 mM HEPES buffer at pH 7.2, and 200 mM background electrolyte concentration. Potential sweeps were from +500 to –200 mV and isosbestic spectral behavior was observed. Spectroelectrochemical data obtained using the Soret bands were used to construct Nernst plots of log [ferri-H-HPX]/[ferro-H-HPX] (or log [ferri-mH-HPX]/[ferro-mH-HPX]) versus applied potential with a slope related to the number of electrons transferred (n) and intercept ([ferri-H-HPX] = [ferro-H-HPX]) corresponding to the mid-point reduction potential, $E_{1/2}$. Here, the redox potentials have not been used to estimate a K_d for the ferro-heme-HPX complexes due to complicating features associated with the redox potentials available for the free heme; e.g., solvent effects, stacking, spin changes, etc.

Cell culture, cell lysis, Western blot and immunoprecipitation analyses

Minimal deviation hepatoma cells (Hepa), derived from the mouse solid tumor BW 7756, were grown in DMEM (Dulbecco's Minimal Essential Medium) supplemented with 2% fetal bovine serum as previously described (Smith and Ledford 1988). For whole cell extract preparation, cells (seeded at 2.5×10^5 cells/well in six-well plates) were cultured for 48 h. These exponentially growing cells were rinsed and incubated in warm, gas-equilibrated, HEPES/NaOH-buffered, serum free DMEM, pH 7.4, with heme-HPX or PBS for the times indicated in the presence or absence of bafilomycin (Sigma Chemical Company) or DMSO. Whole cell extracts were prepared by the addition of cell lysis buffer (100 µl; Cell Signaling Technology Inc., Beverley, MA) to PBS-rinsed cells (ice-cold). After centrifugation (3,000×g for 10 min) of the extract, the protein concentration was determined using the Bicinchoninic acid assay (BCA; Pierce Biotechnology, Rockford, IL) with bovine serum albumin as standard. Proteins in samples of whole cell extracts (20 µg) were resolved on SDS/PAGE gels (15% acrylamide gels) under reducing conditions and the target proteins detected by Western immunoblotting onto polyvinylidene difluoride membranes. The primary antibodies used were anti-rat Heme oxygenase-1 (HO-1) (1:5,000 dilution; antigen: 1–30 amino acid residues; Assay Designs, Ann Arbor, MI) and anti-tubulin (1:2,000 dilution; Santa Cruz Biotechnology Inc., Santa Cruz, CA). The secondary antibodies used were goat anti-mouse Alexa Fluor 680 IgG (Molecular Probes/Invitrogen Corporation, Carlsbad, CA) and goat anti-rabbit IgG IR Dye 800CW (Rockland Immunochemicals, Gilbertsville, PA), respectively, both used at 1:20,000. The blots were scanned with the Odyssey Infrared Imaging System (LI-COR Biosciences, Lincoln, NE) and the signals quantitated by segment analysis using UN-SCAN-IT gel digitizing software (Silk Scientific, Orem, UT, USA). The levels of HO-1 were normalized to tubulin. This experimental series consisted of five individual experiments at 4 h induction and a second set of four at 3 h induction, with two concentrations of bafilomycin (100 or 250 nM).

Results and discussion

We have reconstituted heme-HPX complexes in the form of iron-protoporphyrin IX—hemopexin (H-HPX) and iron-mesoporphyrin IX—hemopexin (mH-HPX) by using HPX to sequester iron-protoporphyrin IX (protoheme) and iron-mesoporphyrin IX (mesoheme), respectively. Spectroelectrochemical measurements were made using the Soret bands for both H-HPX (414 and 428 nm for the oxidized and reduced forms, respectively) and mH-HPX (405 and 412 nm for the oxidized and reduced forms, respectively) at pH 7.2 in aqueous solution containing various background electrolytes. Well-behaved Nernst plots with slopes consistent with a single electron transfer (n = 1) were obtained and representative examples are shown in Fig. 1. Our results obtained in the presence of various background electrolytes are summarized in Table 1. Although the heme binding site of HPX is unique, the $E_{1/2}$ values are in the range reported for other low-spin heme proteins (Gibney 2007), and are consistent with

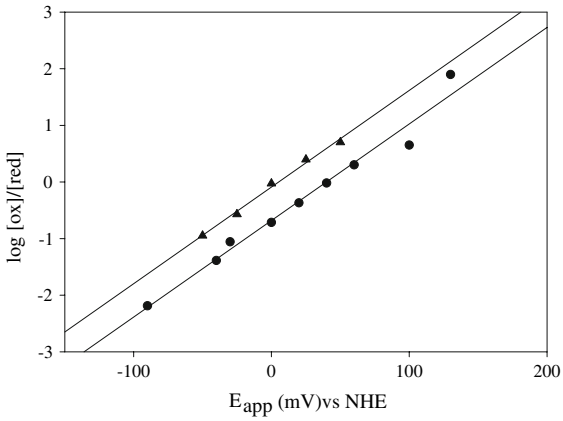

Fig. 1 Nernst plots for the reduction of mH-HPX (▲) and H-HPX (●). Conditions: ▲, 0.1 mM mH-HPX, 0.5 M HEPES (pH 7.2), 0.2 M KCl, and 2.5 mM $K_3Fe(CN)_6$, $E_{1/2}$ = 6 mV; n = 0.99(3); data obtained at λ = 405 nm. ●, 0.08 mM mH-HPX, 0.5 M HEPES (pH 7.2), 0.2 M KCl, and 2.5 mM $K_3Fe(CN)_6$, $E_{1/2}$ = 45 mV; n = 0.99(1); data obtained at λ = 413 nm

the results for HPX isolated from human serum obtained by another method (Hkal et al. 1977).

The observed $E_{1/2}$ values for H-HPX and mH-HPX are sensitive to heme structure and are shifted ~100 mV positive relative to the respective free heme groups. The axial histidine ligands play a major role in controlling redox potentials due to their electronic effects on the metal center. The hydrophobic and reactive vinyl groups of the naturally occurring heme (i.e., iron-protoporphyrin IX) are replaced by ethyl side chains in mH, which makes this heme analog more water soluble. The $E_{1/2}$ values from mH-HPX are lower than those of H-HPX (Table 1), revealing a more stable Fe^{3+} state for this assembly. This is also consistent with previously published observations in the literature where replacement of the vinyl groups on a heme protein with ethyl groups, e.g., the low-spin iron microsomal cytochrome b_5, resulted in a stabilization of the Fe^{3+} form of the protein (i.e., less readily reduced; Reid et al. 1986; Lee et al. 1991).

The influence of cations and anions on the reduction potentials of H-HPX and mH-HPX is seen in the data in Table 1. The origins of the salt effects on $E_{1/2}$ observed here are likely of different origin from the influence of transition metal cations on T_m for heme-HPX (Rosell et al. 2005). Our observations are consistent with the degree to which the surface of the heme molecule is exposed to the solvent (~190 Å^2; Morgan et al. 1976), resulting in an unusually high solvent/environmental accessibility (see depiction of the 3D structure of heme-HPX in Fig. 2). These cation effects on $E_{1/2}$ reflect observations in published melting experiments showing that addition of Na^+ ion increases the melting temperature T_m of both apo- and heme-HPX (Shipulina et al. 2001). Thus, the presence of physiological concentrations of Na^+ increases the stability both of the folded protein itself and its heme pocket as first proposed by Paoli et al. (1999). In the pexin domains of HPX, the central tunnel is lined with carbonyl and amide groups that project in register into the tunnel forming high affinity sites for cations and anions, respectively (Faber et al. 1995; Paoli et al. 1999). One Na^+ and Cl^- also interact with various sites on the surface of the protein at the end of the tunnels, both near and far from the heme site, and hence may explain the significant anion and cation effects on the observed $E_{1/2}$ values. At 200 mM, chloride will slightly stabilize the ferri-heme-HPX complex form. The view of the heme-HPX complex shown in Fig. 2 reveals that the exposed edge of the heme (red) and the sodium (pink) ion in the N-domain are both visible on one side. However, as the heme-HPX complex is rotated around the vertical axis, a phosphate molecule (green) that resides at the edge

Table 1 Redox potentials ($E_{1/2}$) for the hemopexin complexes mH-HPX and H-HPX at pH 7.2 in the presence of various background electrolytes

Hemopexin	Background electrolyte			
	KCl	NaCl	K_2HPO_4	$NaNO_3$
mH-HPX	6	52	23	48
H-HPX	45	88	62	

Conditions: 25°C; 0.03–0.1 mM mH-HPX or H-HPX, 0.5–2.5 mM $K_3Fe(CN)_6$, 0.5 M HEPES and 0.2 M background electrolyte at pH 7.2. $E_{1/2}$ values are in mV relative to NHE and represent the average of at least two independent measurements

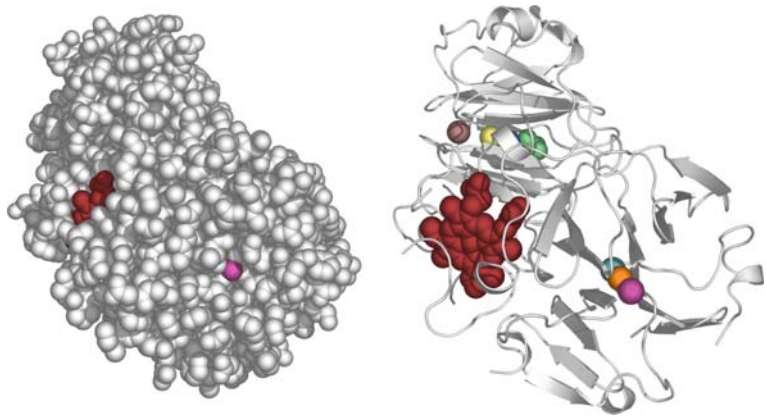

Fig. 2 Structure of heme-hemopexin (*H-HPX*) assembly. Shown are both space filling (LHS) and ribbon (RHS) models, respectively, of heme-hemopexin. The novel heme-binding site is formed between two similar β-propeller domains [N-terminal (lower showing the four blades of the propeller) and C-terminal (*upper*) in these views]. The heme-iron coordinates with two histidine residues (not shown). Sodium and chloride ions are bound in both the central tunnels with a phosphate (*green*) exposed at the surface of the C-domain and a sodium ion (*pink*) exposed in the N-domain. These figures were generated using pdb file 1QHU with PyMol

of a tunnel on the C-terminal domain is observed far from the heme and these other ions. One sodium and two chloride ions are bound within each tunnel and the sodium site is large enough to be occupied by calcium in vivo. Acidic patches formed by conserved Aspartate residues that surround each tunnel opening on both the N- and C- domains potentially provide cation binding sites (Paoli et al. 1999). Extracellular levels of sodium are higher than intracellular levels as in plasma where HPX is needed to bind heme, presumably as ferri-heme. Chloride channels facilitate endosomal acidification and regulate the chloride levels in the endosome (Scheel et al. 2005). Consequently, our observation that the heme-site redox potential is sensitive to the presence of environmental cations and anions is reasonable on both structural and biological grounds.

Since heme-HPX undergoes endocytosis (Smith and Hunt 1990), and endosomes are acidified during their maturation, the heme-HPX complex is exposed to significant pH changes from 7.4 in the plasma to *ca.* 6.5 in early endosomes, 5.5 in the multi-vesicular body and 6.8 in recycling endosome (Clague 1998). Therefore, we also investigated the influence of pH on the formal reduction potential of the heme-HPX assembly using spectroelectrochemistry. pH titrations revealed that the heme-HPX complex is stable over the pH range 6–10 (Cox et al. 1995). At pH less than 5–5.5, HPX does not bind ferri-heme presumably due to protonation of the His_{213} and His_{266} heme coordinating ligands. The $E_{1/2}$ value for mH-HPX at pH 7.2 in the presence of 0.2 M KCl was shifted from 6 to 105 mV on dropping the pH to 5.5. Similar results were obtained for H-HPX. A 100 mV increase in $E_{1/2}$ brought about by a decrease of 1.8 pH units is consistent with a heme-HPX equilibrium reaction involving a single H^+ that stabilizes the reduced form of the ferro-heme-HPX complex. Therefore, we conclude that as the pH is lowered below 6 the ease of Fe^{3+}/Fe^{2+} reduction of the heme-iron within the heme pocket of HPX is increased.

The important role of a decrease in endosomal pH during endocytosis for heme release from HPX for uptake and gene regulation is illustrated by the data in Fig. 3. When acidification of endosomes in cultured cells is blocked by addition of the V-type ATPase inhibitor, bafilomycin (Yoshimori et al. 1991), to the incubation medium, the induction of HO-1 protein by H-HPX (approximately twofold at 3 h and two to threefold at 4 h), detected by immunoblotting, does not occur.

The shift in redox potential observed when heme and mesoheme are sequestered by HPX, and the redox sensitivity of the heme-HPX assembly to electrolyte composition and pH illustrate the importance of first coordination shell (histidine ligation and heme structure) and second coordination shell (protein structure and environment) effects in electron

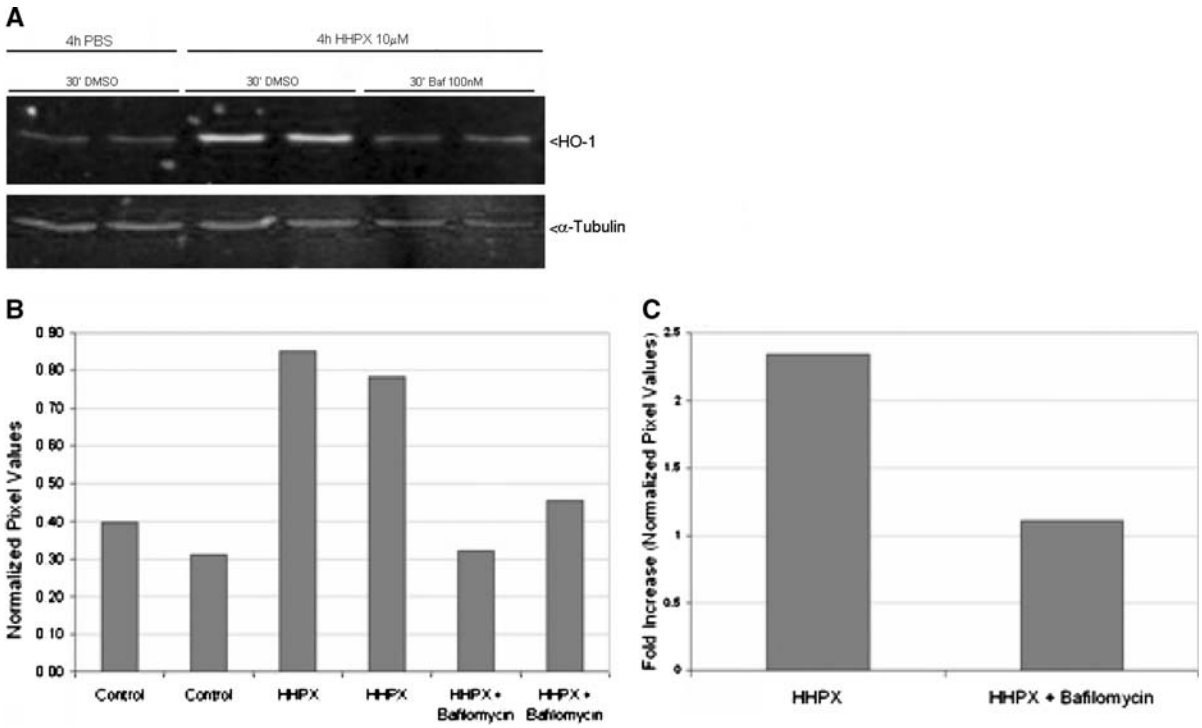

Fig. 3 Bafilomycin prevents induction of heme oxygenase-1 by heme-hemopexin in mouse Hepa cells. Mouse hepatoma cells were incubated with heme-hemopexin (*H-HPX*) for 4 h in the presence and absence of the bafilomycin (100 nM). Bafilomycin or solvent, DMSO, were added to the cell medium 30 min before addition of heme-hemopexin (10 μM) or solvent PBS as indicated in the figure. Whole cell extracts were prepared and HO-1 protein levels detected using Western immunoblotting (*Panel A*) as described in the Methods section, and shown also are HO1 levels normalized to tubulin (*Panel B*) and the average fold induction of HO-1 (*Panel C*). *Data* shown are duplicate samples from a representative experiment from two individual experiments each for 3 or 4 h induction

transfer thermodynamics for the HPX heme transport system. Another soluble heme-binding protein and transporter that interacts with a surface receptor is HasA (heme acquisition system protein A), from the pathogenic bacterium *Serratia marcescens*. This small (Mr 19 kDa) protein, termed a hemophore, differs completely in structure from HPX and binds heme *via* His and Tyr coordination with a $K_d < 10$ nM (Arnoux et al. 1999). Significantly, HasA exhibits a very negative redox potential of –550 mV (Izadi et al. 1997) compared with HPX, similar to mitochondrial c-type cytochromes whose heme is covalently linked to the protein. A critical comparison of HPX and HasA is contained in a recent review (Paoli et al. 2002).

Our observations support, rather than rule out, a possible role for Fe^{3+}-heme/Fe^{2+}-heme redox in facilitating heme release from HPX for uptake into cells. Low pH is a known condition in the early endosomes where the heme is expected to be released from HPX. A drop in pH from 7.2 to 5.5 results in a positive shift in the heme-iron redox potential, suggesting that ease of reduction to the ferro-heme form of HPX may also play a role in heme release from the heme-HPX assembly. There is ample literature precedent to suggest that reduction of ferri-heme to ferro-heme will weaken the iron-imidazole bond (Tabata and Nishimoto 2000), making the imidazole more susceptible to protonation with concomitant bond rupture and subsequent release of heme. Our observations are supported by T_m values at the folded/unfolded half point that are lower for ferro-HPX than the ferri form, indicative of a loss in stability on reduction of the heme-iron (Morgan and Smith 2001; Shipulina et al. 2001; Rosell et al. 2005).

Thus, overall our data support a reductive mechanism for heme delivery to cells from HPX as has been established for redox-active metals like iron and copper whose transport/release is triggered by metal

site reduction associated with metal reductases. See for example iron and copper uptake in yeast *Saccharomyces cerevisiae* (Hassett and Kosman 1995; Askwith and Kaplan 1998; Hassett et al. 2000), the uptake of non-transferrin bound iron into enterocytes *via* DMT1 which involves DCytb, an ascorbate-dependent ferri-reductase that belongs to the cytochrome b561 family, and the uptake of transferrin-bound iron which involves endosomal DMT1 and Steap 3, a flavo-hemoprotein ferri-reductase (Dhungana et al. 2004; McKie 2005; Ohgami et al. 2005). Heme transporters (e.g., HCP1) (Shayeghi et al. 2005) have recently been cloned, but their mechanism of action has not yet been defined. Some utilize energy from ATP hydrolysis; e.g., ABCG2 and ABCB6, a member of the family of ABC transporters (Krishnamurthy et al. 2004, 2006). Another example is the feline leukemia virus receptor subgroup C, FLVCR (Quigley et al. 2004) that is ubiquitously expressed and passively exports heme along a concentration gradient. Current evidence suggests that the heme transporter for heme from HPX is distinctive and differs from HCP1 and FLVCR. Ferri-heme, used as the "substrate" for these heme transporters but not yet proven to be the form of heme transported by them is, however, not an effective competitive inhibitor of heme uptake from [^{59}Fe]heme-HPX; only heme bound to HPX competes with the radioactive complex (Smith and Morgan 1981). Furthermore, the heme from heme-HPX complexes must be rapidly sequestered by the cell since apo-HPX, an avid heme binder, is also not an effective competitive inhibitor (Smith and Morgan 1981).

If reduced heme is generated from ferri-heme-HPX complexes, and ferro-heme may be a transported species, a question arises as to the possible source(s) of electrons for heme-HPX reduction. Proliferating mammalian cells transfer electrons across the plasma membrane from intracellular reductants like NADH to extracellular electron acceptors such as oxygen (Berridge and Tan 1998; Ly and Lawen 2003). This PMET system recycles cytosolic NADH to maintain glycolysis and cell growth, particularly in glycolytic cells (Herst et al. 2004), and can be measured by reduction of the tetrazolium salt, WST-1 (2,(4-iodophenyl)-3-(4-nitrophenyl)-5-(2,4-disulfophenyl)-2H-tetrazolium)), in the presence of an intermediate electron acceptor (IEA; *m*PMS, 1-methoxy-5-methylphenazinium methylsulfate) using the cofactor NADH present in the cell cytosol. The redox potential of heme-HPX places it in a position to accept electrons from ubiquinone implicated in this pathway (Berridge and Tan 2000) and thus heme-HPX complexes would compete with mPMS/WST-1 for electrons from PMET. Such evidence has recently been obtained (Rish et al. 2007), thus implicating heme-HPX as one potential natural substrate for electron transfer across the plasma membrane.

In conclusion, overall the data presented here provide strong evidence that the physical properties of heme-HPX complexes related to ferri-/ferro-heme reduction are both structurally and biologically relevant for heme release from HPX for cellular uptake, intracellular transport of heme and for the regulation of HO-1 expression.

Acknowledgments A.L.C. thanks the National Science Foundation (Grants CHE 0079066 and CHE 0418006) for financial support. M.M.F. is a Duke University Toxicology Program Fellow supported by NIEHS grant T32-ES-07031-21A1. A.S. thanks NIH (Grant DK64363), the American Heart Association and the University of Missouri Research Board for financial support. The authors acknowledge the help of Ms. Rachel Lovelace and Dr. Max Paoli (University of Newcastle, UK) for the generation of the heme-hemopexin structure with PyMol.

References

Alam J, Smith A (1989) Receptor-mediated transport of heme by hemopexin regulates gene expression in mammalian cells. J Biol Chem 264:17637–17640

Alam J, Smith A (1992) Heme-hemopexin-mediated induction of metallothionein gene expression. J Biol Chem 267: 16379–16384

Arnoux P, Haser R, Izadi N, Lecroisey A, Delepierre M, Wandersman C, Czjzek M (1999) The crystal structure of HasA, a hemophore secreted by Serratia marcescens. Nat Struct Biol 6:516–520

Ascenzi P, Bocedi A, Visca P, Altruda F, Tolosano E, Beringhelli T, Fasano M (2005) Hemoglobin and heme scavenging. IUBMB Life 57:749–759

Askwith C, Kaplan J (1998) Iron and copper transport in yeast and its relevance to human disease. Trends Biochem Sci 23:135–138

Beaven GH, Chen S-H, D'Albis A, Gratzer WB (1974) A spectroscopic study of the haemin-human-serum-albumin system. Eur J Biochem 41:539–546

Berridge MV, Tan AS (1998) Trans-plasma membrane electron transport: a cellular assay for NADH- and NADPH-oxidase based on extracellular, superoxide-mediated

reduction of the sulfonated tetrazolium salt WST-1. Protoplasma 205:74–82
Berridge MV, Tan AS (2000) Cell-surface NAD(P)H-oxidase: relationship to trans-plasma membrane NADH-oxidoreductase and a potential source of circulating NADH-oxidase. Antioxid Redox Signal 2:277–288
Clague MJ (1998) Molecular aspects of the endocytic pathway. Biochem J 336:271–282
Conway TP, Morgan WT, Liem HH, Muller-Eberhard U (1975) Catabolism of photo-oxidized and desialylated hemopexin in the rabbit. J Biol Chem 250:3067–3073
Cox MC, Le Brun N, Thomson AJ, Smith A, Morgan WT, Moore GR (1995) MCD, EPR and NMR spectroscopic studies of rabbit hemopexin and its heme binding domain. Biochim Biophys Acta 1253:215–223
Davies DM, Smith A, Muller-Eberhard U, Morgan WT (1979) Hepatic subcellular metabolism of heme from heme-hemopexin: incorporation of iron into ferritin. Biochem Biophys Res Commun 91:1504–1511
Dhungana S, Crumbliss AL (2007) Uv-visible spectroelectrochemsitry of selected iron containing proteins. In: Kaim WK, Klein A (eds) Spectroelectrochemistry. Royal Society of Chemistry, Cambridge, UK (in press)
Dhungana S, Taboy CH, Zak O, Larvie M, Crumbliss AL, Aisen P (2004) Redox properties of human transferrin bound to its receptor. Biochemistry 43:205–209
Eskew JD, Vanacore RM, Sung L, Morales PJ, Smith A (1999) Cellular protection mechanisms against extracellular heme. heme- hemopexin, but not free heme, activates the n-terminal c-jun kinase. J Biol Chem 274:638–648
Faber HR, Groom CR, Baker HM, Morgan WT, Smith A, Baker EN (1995) 1.8 Angstrom crystal-structure of the C-terminal domain of rabbit serum hemopexin. Structure 3:551–559
Genco CA, Dixon DW. Emerging strategies in microbial haem capture. Mol Microbiol 39:1–11
Gibney B (2007) Heme-protein database. http://heme.chem.columbia.edu/heme.php
Gutteridge JM, Smith A (1988) Antioxidant protection by haemopexin of haem-stimulated lipid peroxidation. Biochem J 256:861–865
Halliwell B, Gutteridge JMC (1986) Iron and free radical reactions: two aspects of antioxidant protection. Trends Biochem Sci 11:372–375
Hassett R, Dix DR, Eide DJ, Kosman DJ (2000) The Fe(II) permease Fet4p functions as a low affinity copper transporter and supports normal copper trafficking in Saccharomyces cerevisiae. Biochem J 351:477–484
Hassett R, Kosman DJ (1995) Evidence for Cu(II) reduction as a component of copper uptake by Saccharomyces cerevisiae. J Biol Chem 270:128–134
Herst PM, Tan AS, Scarlett DJ, Berridge MV (2004) Cell surface oxygen consumption by mitochondrial gene knockout cells. Biochim Biophys Acta 1656:79–87
Hkal Z, Suttnar J, Vodrazka Z (1977) Redox potential of human serum haemopexin. Stud Biophys (Berlin) 63:55–58
Hkal Z, Vodrazka Z, Kalousek I (1974) Transfer of heme from ferrihemoglobin and ferrihemoglobin isolated chains to hemopexin. Eur J Biochem 43:73–78
Izadi N, Henry Y, Haladjian J, Goldberg ME, Wandersman C, Delepierre M, Lecroisey A (1997) Purification and characterization of an extracellular heme-binding protein, HasA, involved in heme iron acquisition. Biochemistry 36:7050–7057
Krishnamurthy P, Ross DD, Nakanishi T, Bailey-Dell K, Zhou S, Mercer K, Sarkadi EB, Sorrentino BP, Schuetz JD (2004) The stem cell marker Bcrp/ABCG2 enhances hypoxic cell survival through interactions with heme. J Biol Chem 279:24218–24225
Krishnamurthy PC, Du G, Fukuda Y, Sun D, Sampath J, Mercer KE, Wang J, Sosa-Pineda B, Murti GP, Schuetz JD (2006) Identification of a mammalian porphyrin transporter. Nature 443:586–589
Lee K-B, Jun E, LaMar GN, Rezzano I, Pandey RK, Smith KM, Walker FA, Buttlaire DH (1991) Influence of heme vinyl- and carboxylate-protein contacts on structure and redox properties of bovine cytochrome b. J Am Chem Soc 113:3576–3583
Liem HH, Spector JI, Conway TP, Morgan WT, Muller-Eberhard U (1975) Effect of hemoglobin and hematin on plasma clearance of hemopexin, photo-inactivated hemopexin and albumin. Proc Soc Exp Biol Med 148: 519–522
Ly JD, Lawen A (2003) Transplasma membrane electron transport: enzymes involved and biological function. Redox Rep 8:3–21
McKie AT (2005) A ferrireductase fills the gap in the transferrin cycle. Nat Genet 37:1159–1160
Miller YI, Smith A, Morgan WT, Shaklai N (1996) Role of hemopexin in protection of low-density lipoprotein against hemoglobin-induced oxidation. Biochemistry 35:13112–13117
Morgan WT, Liem HH, Sutor RP, Muller-Eberhard U (1976) Transfer of heme from heme-albumin to hemopexin. Biochim Biophys Acta 444:435–445
Morgan WT, Muller-Eberhard U (1972) Interactions of porphyrins with rabbit hemopexin. J Biol Chem 247:7181–7187
Morgan WT, Muster P, Tatum F, Kao SM, Alam J, Smith A (1993) Identification of the histidine residues of hemopexin that coordinate with heme-iron and of a receptor-binding region. J Biol Chem 268:6256–6262
Morgan WT, Muster P, Tatum FM, McConnell J, Conway TP, Hensley P, Smith A (1988) Use of hemopexin domains and monoclonal antibodies to hemopexin to probe the molecular determinants of hemopexin-mediated heme transport. J Biol Chem 263:8220–8225
Morgan WT, Smith A (1984) Domain structure of rabbit hemopexin. Isolation and characterization of a heme-binding glycopeptide. J Biol Chem 259:12001–12006
Morgan WT, Smith A (2001) Binding and transport of iron-porphyrins by hemopexin. Adv Inorg Chem 51: 205–241
Ohgami RS, Campagna DR, Greer EL, Antiochos B, McDonald A, Chen J, Sharp JJ, Fujiwara Y, Barkers JE, Fleming MD (2005) Identification of a ferrireductase required for efficient transferrin-dependent iron uptake in erythroid cells. Nat Genet 37:1264–1269
Paoli M, Anderson BF, Baker HM, Morgan WT, Smith A, Baker EN (1999) Crystal structure of hemopexin reveals a novel high-affinity heme site formed between two β propeller domains. Nat Struct Biol 6:926–931

Paoli M, Marles-Wright J, Smith A (2002) Structure-function relationships in heme-proteins. DNA Cell Biol 21:271–280

Quigley JG, Yang Z, Worthington MT (2004) Identification of a human heme exporter that is essential for erythropoiesis. Cell 118:757–766

Reid LS, Lim AR, Mauk AG (1986) Role of heme vinyl groups in cytochrome b5 electron transfer. J Am Chem Soc 108:8197–8201

Rish K, Swartzlander R, Sadikot T, Berridge MV, Smith A (2007) Interaction of heme and heme-hemopexin with an extracellular oxidant system used to measure cell growth-associated plasma membrane electron transport. Biochim Biophys Acta http://dx.doi9.org/10.1016/j.bbabio.2007.06.03

Rosell FI, Mauk MR, Mauk AG (2005) pH and metal ion-induced stability of the hemopexin-heme complex. Biochemistry 44:1872–1879

Scheel O, Zdebik AA, Lourdel S, Jentsch TJ (2005) Voltage dependent electrogenic chloride/proton exchange by endosomal CLC proteins. Nature 436:424–427

Seery VL, Morgan WT, Muller-Eberhard U (1975) Interaction of rabbit hemopexin with rose bengal and photooxidation of the rose bengal-hemopexin complex. J Biol Chem 250:6439–6444

Shayeghi M, Latunde-Dada GO, Oakhill JS (2005) Identification of an intestinal heme transporter. Cell 122:789–801

Shipulina N, Smith A, Morgan WT (2001) Effects of reduction and ligation of heme iron on the thermal stability of heme-hemopexin complexes. J Protein Chem 20:145–154

Smith A, Eskew JD, Borza CM, Pendrak M, Hunt RC (1997) Role of heme-hemopexin in human T-lymphocyte proliferation. Exp Cell Res 232:246–254

Smith A, Hunt RC (1990) Hemopexin joins transferrin as representative members of a distinct class of receptor-mediated endocytic transport systems. Eur J Cell Biol 53:234–245

Smith A, Ledford BE (1988) Expression of the haemopexin-transport system in cultured mouse hepatoma cells. Links between haemopexin and iron metabolism. Biochem J 256:941–950

Smith A, Morgan WT (1978) Transport of heme by hemopexin to the liver: evidence for receptor-mediated uptake. Biochem Biophys Res Commun 84:151–157

Smith A, Morgan WT (1979) Haem transport to the liver by haemopexin. Receptor-mediated uptake with recycling of the protein. Biochem J 182:47–54

Smith A, Morgan WT (1981) Hemopexin mediated transport of heme into isolated rat hepatocytes. J Biol Chem 256:10902–10909

Smith A, Morgan WT (1984) Hemopexin-mediated heme uptake by liver. Characterization of the interaction of heme-hemopexin with isolated rabbit liver plasma membranes. J Biol Chem 259:12049–12053

Sung L, Womack M, Shipulina N, Morales P, Smith A (2000) Cell surface events for metallothionein-1 and heme oxygenase-1 regulation by the hemopexin heme transport system. Antioxid Redox Signal 2:753–765

Tabata M, Nishimoto J (2000) Equilibrium data of porphyrins and metalloporphyrins. In: Kadish KM, Smith KM, Guilard R (eds) The porphyrin handbook, database of redox potentials and binding constants. Academic Press, NY, pp 221–419

Taboy CH, Bonaventura C, Crumbliss AL (2002) Anaerobic oxidations of myoglobin and hemoglobin using spectroelectrochemistry. In: Sen CK, Packer L, Vol Eds, Abelson JN, Simon MI (eds-in-chief) Methods in enzymology—Redox cell biology and genetics. Academic Press, NY, pp 187–209

Tolosano E, Fagoonee S, Hirsch E, Berger FG, Baumann H, Silengo L, Altruda F (2002) Enhanced splenomegaly and severe liver inflammation in haptoglobin/hemopexin double-null mice after acute hemolysis. Blood 100:4201–4208

Tolosano E, Hirsch E, Patrucco E, Camaschella C, Navone R, Silengo L, Altruda F (1999) Blood defective recovery and severe renal damage after acute hemolysis in hemopexin-deficient mice. Blood 94:3906–3914

Vanacore R, Eskew J, Morales P, Sung L, Smith A (2000) Role for copper in transient oxidation and nuclear translocation of MTF-1, but not of NFkB, by the hemopexin heme transport system. Antioxid Redox Signal 2:739–752

Yoshimori T, Yamamoto A, Moriyama Y, Futai M, Tashir Y (1991) Bafilomycin a1, a specific inhibitor of vacuolar-type H(+)-ATPase, inhibits acidification and protein degradation in lysosomes of cultured cells. J Biol Chem 266:17707–17712